Letter

3D Localization for Multiple AUVs in Anchor-Free Environments by Exploring the Use of Depth Information

Yichen Li, *Member, IEEE*, Wenbin Yu, *Member, IEEE*, and Xinping Guan, *Fellow, IEEE*

Dear Editor,

This letter investigates the cooperative localization problem for multiple autonomous underwater vehicles (AUVs) in underwater anchor-free environments, where AUV localization errors grow without bound due to the accumulated errors in inertial measurements (termed accumulated errors hereafter) and the lack of anchors (with known positions). Different from previous works, this letter is based on a message-passing distributed framework and the designed algorithm improves the localization accuracy mainly by the cooperation among AUVs and the use of depth information to mitigate the influence of the accumulated errors and harsh environments. Through simulations, the advantages of the proposed algorithm are verified by comparisons with different state-of-the-art alternative methods.

With the development of AUV technologies, multiple-AUV (multi-AUV) cooperative task execution has gradually become a trend [1]. However, due to the complex underwater environments, AUV localization has always been a challenging problem [2]. Usually, it is achieved with the assistance of anchors to obtain position reference information. Considering the limited coverage of current deployed underwater networks, AUVs should often work in anchor-free environments [3], and the error accumulation in inertial measurements would make localization errors grow unbounded [4]. Under these circumstances, cooperation could be applied to improve the localization accuracy by exchanging information among AUVs [5]. Recently, cooperative localization methods have been designed [3], [6], [7], among which belief propagation (BP) is commonly used for underwater scenarios due to its distributed nature and low complexity. Moreover, its extensions [8], [9] have verified their advantages in non-Gaussian nonlinear problems. However, most works rely on anchors to achieve accuracy improvement. In anchor-free environments, works [3], [10], [11] try to alleviate the localization degradation for AUVs by modifying the use of yaw angles. Although the designed strategies can also be applied to pitch angles, the method designed specifically for the error accumulation in them is still lacking.

In underwater anchor-free environments, in addition to inertial measurements, the depth is the only available absolute information that can be directly measured on board. Usually, depth measurements are used to correct the predicted AUV depths [3]. Furthermore, with known depth information, many works have treated localization as a 2-dimensional (2D) problem [12]. However, such a simplification cannot reflect the true conditions of the ocean [13]. Since depth measurements could be proprioceptively obtained and do not contain accumulated errors, considering the information scarcity in anchor-free scenarios, exploring the use of depth measurements could be a viable way to improve the localization accuracy of AUVs.

Corresponding author: Wenbin Yu.

Citation: Y. C. Li, W. B. Yu, and X. P. Guan, "3D localization for multiple AUVs in anchor-free environments by exploring the use of depth information," *IEEE/CAA J. Autom. Sinica*, 2023, DOI: 10.1109/JAS.2023.123261

The authors are with the Department of Automation, Shanghai Jiao Tong University, Shanghai 200240, and also with the Key Laboratory of System Control and Information Processing, Ministry of Education of China, Shanghai Jiao Tong University, Shanghai 200240, China (e-mail: liyichensjtu@sjtu.edu.cn; yuwenbin@sjtu.edu.cn; xpguan@sjtu.edu.cn).

Color versions of one or more of the figures in this paper are available online at http://ieeexplore.ieee.org.

Digital Object Identifier 10.1109/JAS.2023.123261

This letter aims to improve the localization accuracy of multiple AUVs by designing a distributed cooperative localization algorithm, named cooperative localization aided by depth information (CLADI). The contributions of this letter are as follows: 1) In the designed position prediction, the misleading of the accumulated errors is corrected using depth measurements from different timesteps. 2) The accuracy of relative information between AUVs is improved by compressing the particle coverage using depth information, and the proposed transmitted messages could adapt to the harsh underwater environments, such as sounding ray bending, asynchronization, etc.

System model: A group of N AUVs are considered, whose labels are contained in set $\mathcal{A}=\{1,\ldots,N\}$. The position variables of AUVs are modeled as $\boldsymbol{x}_i^{(t)}=[x_i^{(t)},y_i^{(t)},z_i^{(t)}]^T$ ($\mathbf{x}_i^{(t)}=[\mathrm{x}_i^{(t)},\mathrm{y}_i^{(t)},\mathrm{z}_i^{(t)}]^T$ for particles), where $i\in\mathcal{A}$ is the AUV index, (t) denotes timestep.

As mobile vehicles, AUV localization usually involves a position prediction process that is based on the inertial measurements

$$\hat{\boldsymbol{x}}_i^{(-,t)}=g(\hat{\boldsymbol{x}}_i^{(t-1)},\boldsymbol{I}_i^{(t-1)}),\quad i\in\mathcal{A} \tag{1}$$

where symbols ^ and − respectively indicate the estimated and predicted outputs, $\boldsymbol{I}_i^{(t-1)}=\{\hat{v}_i^{(t-1)},\hat{\theta}_i^{(t-1)},\hat{\gamma}_i^{(t-1)}\}$ denotes the inertial measurements that contain speed $\hat{v}_i^{(t-1)}$, yaw $\hat{\theta}_i^{(t-1)}$ and pitch $\hat{\gamma}_i^{(t-1)}$. In addition, the models of the inertial measurements are

$$\hat{v}_i^{(t)}=v_i^{(t)}+\mu_i^{(t)},\quad \hat{\theta}_i^{(t)}=\theta_i^{(t)}+\xi_i^{(t)},\quad i\in\mathcal{A} \tag{2}$$

$$\hat{\gamma}_i^{(t)}=\gamma_i^{(t)}+\sum_{\tau=1}^{t}\epsilon_i^{(\tau)},\quad i\in\mathcal{A} \tag{3}$$

where $\mu_i^{(t)}$, $\xi_i^{(t)}$ and $\epsilon_i^{(t)}$ are zero-mean Gaussian noises with variances $\sigma_{v,i}^2$, $\sigma_{\theta,i}^2$ and $\sigma_{\gamma,i}^2$, respectively. Considering speeds could be measured with high accuracy using the Doppler velocity log and the treatments for the accumulated errors in yaw and pitch angles are often similar, only the error accumulation in pitch angles is shown since it could be further corrected by depth information.

Moreover, we consider the models of depth measurements $\hat{z}_i^{(t)}$ and relative distance measurements $\hat{d}_{j\to i}^{(t)}$ as

$$\hat{z}_i^{(t)}=z_i^{(t)}+\varrho_i^{(t)},\quad i\in\mathcal{A} \tag{4}$$

$$\hat{d}_{j\to i}^{(t)}=d_{j\to i}^{(t)}+\zeta_{j\to i}^{(t)},\quad i,\ j\in\mathcal{A} \tag{5}$$

$$=\left\|\boldsymbol{x}_j^{(t)}-\boldsymbol{x}_i^{(t)}\right\|+\zeta_{j\to i}^{(t)},\quad i,\ j\in\mathcal{A} \tag{6}$$

where $\varrho_i^{(t)}$ and $\zeta_{j\to i}^{(t)}$ are zero-mean Gaussian noises with variances $\sigma_{z,i}^2$ and $\sigma_{d,i}^2$, respectively, function $\|\cdot\|$ calculates the Euclidean distance, and the subscript $j\to i$ indicates the measured distance is between the jth and ith AUVs and used for the localization of the ith AUV. Note that the designed CLADI is particle-based and could be used for various noise models, not limited to Gaussian [11].

Algorithm design: In this part, we introduce the proposed CLADI algorithm. It is designed based on BP, and the so-called belief is an estimate of the position distribution of AUV. The belief $b_i^{(t)}(\boldsymbol{x}_i^{(t)})$ of the ith AUV at the timestep (t) is defined as

$$b_i^{(t)}(\boldsymbol{x}_i^{(t)})\propto p_i^{(t)}(\boldsymbol{x}_i^{(t)})\prod_{j\in\mathcal{N}_i}m_{j\to i}^{(t)}(\boldsymbol{x}_i^{(t)}),\quad i\in\mathcal{A} \tag{7}$$

where $\propto$ denotes a proportional relationship, $\mathcal{N}_i$ indicates the neighbors that could establish communication with the ith AUV, $p_i^{(t)}(\boldsymbol{x}_i^{(t)})$ is the prior position distribution (termed the prior), and $m_{j\to i}^{(t)}(\boldsymbol{x}_i^{(t)})$ denotes the message transmitted from the jth AUV to the ith AUV.

In AUV localization, the prior $p_i^{(t)}(\boldsymbol{x}_i^{(t)})$ is usually predicted with inertial measurements according to (1) as

$$p_i^{(t)}(\boldsymbol{x}_i^{(t)})=\int p(\boldsymbol{x}_i^{(t)}|\boldsymbol{x}_i^{(t-1)},\boldsymbol{I}_i^{(t-1)},\hat{z}_i^{(t-1:t)})b_i^{(t-1)}(\boldsymbol{x}_i^{(t-1)})\times p(\boldsymbol{I}_i^{(t-1)})p(\hat{z}_i^{(t-1:t)})\,d\boldsymbol{x}_i^{(t-1)}d\boldsymbol{I}_i^{(t-1)}d\hat{z}_i^{(t-1:t)} \tag{8}$$

where $p(\boldsymbol{x}_i^{(t)}|\boldsymbol{x}_i^{(t-1)},\boldsymbol{I}_i^{(t-1)},\hat{z}_i^{(t-1:t)})$ is a statistical version of (1), $p(\boldsymbol{I}_i^{(t-1)})$ and $p(\hat{z}_i^{(t-1:t)})$ represent likelihood functions.

Based on the aforementioned distance measurement model, the message $m_{j\to i}^{(t)}(\boldsymbol{x}_i^{(t)})$ expresses the position information of the ith AUV from the perspective of the jth AUV and is defined as

$$m_{j\to i}^{(t)}(\boldsymbol{x}_i^{(t)}) \propto \int p(\hat{d}_{j\to i}^{(t)}|\boldsymbol{x}_j^{(t)},\boldsymbol{x}_i^{(t)}) b_j^{(t)}(\boldsymbol{x}_j^{(t)})\, d\boldsymbol{x}_j^{(t)} \tag{9}$$

where $p(\hat{d}_{j\to i}^{(t)}|\boldsymbol{x}_j^{(t)},\boldsymbol{x}_i^{(t)})$ is the likelihood function.

Thus, with the obtained messages, AUVs could locally calculate their own beliefs by multiplication as in (7). Thus, the performance of CLADI largely depends on whether the prior and the messages can accurately express the position information. In the following, particle-realized prior and message are designed to obtain higher information accuracy as well as better environmental adaptability.

The prior: Since inertial measurements are used in the prediction process, the design of the prior is the key to alleviate the localization accuracy degradation caused by the accumulated errors.

Assuming the output belief of the ith AUV at the timestep $(t-1)$ is represented by K weighted particles $\{\boldsymbol{x}_{b,k,i}^{(t-1)}, w_{b,k,i}^{(t-1)}\}_{k=1}^{K}$, the particles $\boldsymbol{x}_{p,k,i}^{(t)}$ of the prior at the timestep (t) can be predicted as

$$\begin{aligned}
&x_{p,k,i}^{(t)} = x_{b,k,i}^{(t-1)} + v_k \tau \cos(\gamma_k)\sin(\theta_k)\\
&y_{p,k,i}^{(t)} = y_{b,k,i}^{(t-1)} + v_k \tau \cos(\gamma_k)\cos(\theta_k)\\
&z_{p,k,i}^{(t)} = z_k,\ \ z_k \sim \mathcal{N}(\hat{z}_i^{(t)}, \sigma_{z,i}^2),\ \ v_k \sim \mathcal{N}(\hat{v}_i^{(t-1)}, \sigma_{v,i}^2)\\
&\theta_k \sim \mathcal{N}(\hat{\theta}_i^{(t-1)}, \sigma_{\theta,i}^2),\quad \gamma_k \sim \mathcal{N}(\hat{\varphi}_i^{(t-1)}, (\sigma_{\varphi,i}^{(t-1)})^2)
\end{aligned} \tag{10}$$

where τ is the duration between two adjacent timesteps, $z_k \sim \mathcal{N}(\cdot)$ denotes z_k follows a Gaussian distribution. In (10), since $\hat{z}_i^{(t)}$, $\hat{v}_i^{(t-1)}$ and $\hat{\theta}_i^{(t-1)}$ can be directly measured, the corresponding particles are sampled from the measurements. However, due to the accumulated errors in pitch measurements, an angle $\hat{\varphi}_i^{(t-1)}$ corrected with depth information is used instead, which is calculated as

$$\hat{\varphi}_i^{(t-1)} = \arcsin \frac{\hat{z}_i^{(t)} - \hat{z}_i^{(t-1)}}{\hat{v}_i^{(t-1)}\tau}. \tag{11}$$

Since depth measurements do not contain accumulated errors, the use of $\hat{\varphi}_i^{(t-1)}$ would significantly alleviate the influence of the error accumulation in $\hat{\gamma}_i^{(t)}$. Moreover, $\sigma_{\varphi,i}^{(t)} = \sigma_{\varphi,i}^{(t-1)} + \Delta\sigma_i$ is designed in an additive manner to cope with the uncertainty accumulation during navigation, and $\Delta\sigma_i$ simulates the accumulated uncertainty.

Since the particles in $\{\boldsymbol{x}_{b,k,i}^{(t-1)}, w_{b,k,i}^{(t-1)}\}_{k=1}^{K}$ are equally treated, the corresponding weights remain unchanged $w_{p,k,i}^{(t)} = w_{b,k,i}^{(t-1)}$. In this way, the particles $\{\boldsymbol{x}_{p,k,i}^{(t)}, w_{p,k,i}^{(t)}\}_{k=1}^{K}$ of the prior are obtained.

The message: In CLADI, the *message* indicates the relative position information between AUVs. In this part, the designed *message* improves the information accuracy by compressing the particle distribution with depth measurements. It is also able to overcome the measurement bias caused by the bending of sound rays, asynchronization between AUVs, etc.

Assuming the prior $p_j^{(t)}$ and the message $m_{j\to i}^{(t)}$ are represented by $\{\boldsymbol{x}_{p,k,j}^{(t)}, w_{p,k,j}^{(t)}\}_{k=1}^{K}$ and $\{\boldsymbol{x}_{m,k,j\to i}^{(t)}, w_{m,k,j\to i}^{(t)}\}_{k=1}^{K}$, respectively, with the relative distance $\hat{d}_{j\to i}^{(t)}$, the traditional way of the message generation for 3D localization is as follows:

$$\begin{aligned}
&x_{m,k,j\to i}^{(t)} = x_{p,k,j}^{(t)} + d_k \cos(\alpha_k)\sin(\beta_k),\ \ \alpha_k \sim \mathcal{U}(0,2\pi)\\
&y_{m,k,j\to i}^{(t)} = y_{p,k,j}^{(t)} + d_k \cos(\alpha_k)\cos(\beta_k)\ \ \beta_k \sim \mathcal{U}(0,2\pi)\\
&z_{m,k,j\to i}^{(t)} = z_{p,k,j}^{(t)} + d_k \sin(\alpha_k),\ \ d_k \sim \mathcal{N}(\hat{d}_{j\to i}^{(t)}, \sigma_{d,i}^2).
\end{aligned} \tag{12}$$

Since no direction is involved, α_k and β_k are uniformly distributed with $\mathcal{U}(0,2\pi)$, and the generated particles would cover a sphere.

With the depth measurements of both the ith and jth AUVs, the particle distribution can be compressed into a ring,

$$\begin{aligned}
&x_{m,k,j\to i}^{(t)} = x_{p,k,j}^{(t)} + d_k \sin(\beta_k),\ \ \beta_k \sim \mathcal{U}(0,2\pi)\\
&y_{m,k,j\to i}^{(t)} = y_{p,k,j}^{(t)} + d_k \cos(\beta_k),\ \ z_k \sim \mathcal{N}(\hat{z}_i^{(t)}, \sigma_{z,i}^2)\\
&z_{m,k,j\to i}^{(t)} = z_k,\ \ d_k \sim \mathcal{N}(\sqrt{(\hat{d}_{j\to i}^{(t)})^2 + (\hat{z}_j^{(t)} - \hat{z}_i^{(t)})^2}, \sigma_{d,i}^2).
\end{aligned} \tag{13}$$

In this way, with the same number of particles, a much smaller area needs to be covered and, accordingly, the distance between adjacent particles has been narrowed, leading to higher representation resolution of the relative position information.

To further explore the available information, a rough direction from the jth AUV to the ith AUV can be obtained.

$$\hat{\phi}_{j\to i}^{(t)} = \begin{cases} \rho\ , & \hat{x}_j^{(-,t)} > \hat{x}_i^{(-,t)} \text{ and } \hat{y}_j^{(-,t)} > \hat{y}_i^{(-,t)}\\ \pi - \rho, & \hat{x}_j^{(-,t)} > \hat{x}_i^{(-,t)} \text{ and } \hat{y}_j^{(-,t)} \le \hat{y}_i^{(-,t)}\\ -\rho, & \hat{x}_j^{(-,t)} \le \hat{x}_i^{(-,t)} \text{ and } \hat{y}_j^{(-,t)} > \hat{y}_i^{(-,t)}\\ \rho - \pi, & \hat{x}_j^{(-,t)} \le \hat{x}_i^{(-,t)} \text{ and } \hat{y}_j^{(-,t)} \le \hat{y}_i^{-,(t)} \end{cases} \tag{14}$$

where $\rho = \arcsin \frac{\|\hat{x}_j^{(-,t)} - \hat{x}_i^{(-,t)}\|_2}{\sqrt{(\hat{x}_j^{(-,t)} - \hat{x}_i^{(-,t)})^2 + (\hat{y}_j^{(-,t)} - \hat{y}_i^{(-,t)})^2}}$. The predicted positions $\hat{\boldsymbol{x}}_j^{(-,t)}$ and $\hat{\boldsymbol{x}}_i^{(-,t)}$ can be calculated by averaging the weighted particles of the *priors* of AUVs. With the rough direction $\hat{\phi}_{j\to i}^{(t)}$, the particle distribution in (13) can be further compressed by replacing the direction particles β_k with

$$\beta_k \sim \mathcal{U}\Big(\hat{\phi}_{j\to i}^{(t)} - \frac{1}{2}\vartheta, \hat{\phi}_{j\to i}^{(t)} + \frac{1}{2}\vartheta\Big) \tag{15}$$

where ϑ is designed to alleviate the influence of the uncertainties brought by the rough direction $\hat{\phi}_{j\to i}^{(t)}$.

Moreover, to overcome the distance measurement bias, a time-varying compensation $c_{j\to i}^{(t)}$ for $\hat{d}_{j\to i}^{(t)}$ is designed as

$$c_{j\to i}^{(t)} = \begin{cases} c_{j\to i}^{(t-1)} - \Delta c_{j\to i},\ \hat{d}_{j\to i}^{(t)} - c_{j\to i}^{(t-1)} \le \|\hat{\boldsymbol{x}}_j^{(t)} - \hat{\boldsymbol{x}}_i^{(t)}\| \\ c_{j\to i}^{(t-1)} + \Delta c_{j\to i},\ \hat{d}_{j\to i}^{(t)} - c_{j\to i}^{(t-1)} > \|\hat{\boldsymbol{x}}_j^{(t)} - \hat{\boldsymbol{x}}_i^{(t)}\|. \end{cases} \tag{16}$$

It can be seen that the value of $c_{j\to i}^{(t)}$ varies with measurements and position estimates. If the compensated distance $(\hat{d}_{j\to i}^{(t)} - c_{j\to i}^{(t-1)})$ is smaller than the calculated value $\|\hat{\boldsymbol{x}}_j^{(t)} - \hat{\boldsymbol{x}}_i^{(t)}\|$, it means the current compensation is too big and should be decreased.

Furthermore, a similar approach in (15) is applied to generate the distance particles d_k

$$\begin{aligned}
&d_k \sim \mathcal{U}\Big(\hat{d} - \frac{1}{2}\iota, \hat{d} + \frac{1}{2}\iota\Big)\\
&\hat{d} = \sqrt{(\hat{d}_{j\to i}^{(t)} - c_{j\to i}^{(t-1)})^2 + (\hat{z}_j^{(t)} - \hat{z}_i^{(t)})^2}
\end{aligned} \tag{17}$$

where ι is also used to overcome the uncertainties caused by measurement biases and errors. The main idea that we extend the coverage of particles with (15) and (17) is that we would like to ensure part of the particles could be distributed near the true value even under the condition of unknown biases and errors. When the *messages* multiply as in (7), the particles near the true value would obtain higher weights and dominate the localization results. In this way, the influence of biases and errors can be alleviated.

By replacing the distance and direction particles in (13) with (15) and (17), the proposed message is obtained. Then, the belief can be calculated as (7). Details are described in [11].

Simulation results: In this part, we validate the proposed CLADI algorithm through various simulations, where two $600\times600\times400$ m^3 scenarios are considered. In the first scenario, four anchors and a single AUV is involved to validate the effectiveness of the proposed message. The use of anchors is to avoid the influence of the accumulated errors. In the second scenario, four AUVs are used to compare the localization accuracy of CLADI with state-of-the-art alternative methods. In both scenarios, the speeds of AUVs are set to 5 m/s and the duration of navigation is 100 s. The variances of yaw, pitch, speed, depth, and distance measurements are 0.1, 12, 0.1, 1, and 4, respectively. The number of used particles is 200. The localization

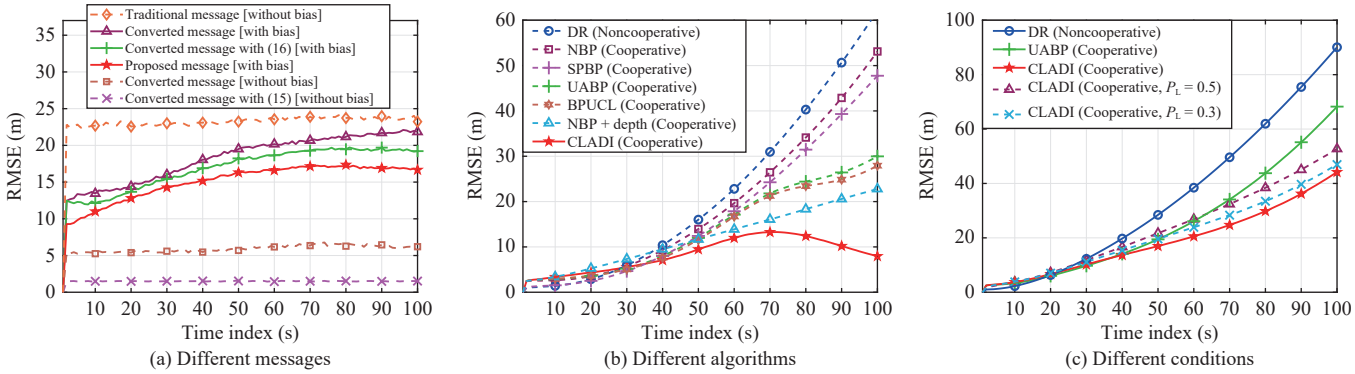

(a) Different messages (b) Different algorithms (c) Different conditions

Fig. 1. RMSE comparisons.

accuracy is measured by root-mean-square errors (RMSEs), which are calculated through 1000 Monte-Carlo runs.

In Fig. 1(a), different messages and two conditions, with or without measurement bias, are applied to validate the advantages of the proposed messages. The traditional message is generated with (12), and the converted message is a compressed version using depth measurements with (13). Fig. 1(a) also demonstrates the effectiveness of (15)−(17) in the message design. When the measurement bias is not considered, the converted message enjoys a clear advantage compared with the traditional one due to higher particle resolution. In addition, the rough direction brought by (15) further reduces the coverage requirement of the message and accordingly improves the relative position information accuracy. Under the measurement-bias condition, the initial biases are set within 20 m and randomly grow with time. By involving the bias compensation (16), the error growth is alleviated. Moreover, through condensing the particle coverage and compensating the measurement bias, the proposed message, generated based on (15) and (17), could provide the best localization accuracy.

In Fig. 1(b), the localization accuracy of different algorithms is shown. Dead-reckoning (DR) is noncooperative and directly uses inertial measurements to predict position estimates, which are seriously misled by the accumulated errors. Compared with DR, nonparametric BP (NBP) [8] and sigma point BP (SPBP) [9] improve localization accuracy by cooperation among AUVs. However, since the accumulated errors are not specifically considered, the improvement is limited. By involving depth measurements and the design in (11), a clear accuracy improvement of NBP is achieved and proves the validity of our design. In BPUCL [3] and UABP [10], the accumulated errors have been dealt with by compensation and expanding the particle coverage of the prior. However, the use of depth is not fully exploited. In CLADI, the proposed prior applies the pitch angle corrected with depth measurements and avoids the impact of accumulated errors. Combined with a growing particle coverage, CLADI provides the best localization accuracy compared with the aforementioned methods.

To further validate CLADI in practical uses, Fig. 1(c) shows the localization performance when the accumulated errors are contained in both yaw and pitch measurements. Moreover, packet-loss conditions are also involved to simulate the effect of harsh communication environments and network changes, where P_L denotes the probability that an AUV loses all the messages. As a result, the accuracy drop of CLADI is limited and it still provides better accuracy compared with others even under harsh conditions ($P_L = 0.5$ indicates the packet-loss probability of each communication reaches 0.8).

Conclusion: In this letter, multi-AUV cooperative localization in 3D anchor-free environments has been studied and a distributed message-passing localization algorithm named CLADI is proposed. In CLADI, the accumulated errors in pitch angles are corrected using depth measurements, leading to higher prediction accuracy. Depth information is also used to improve the relative position accuracy by compressing the space among particles. Moreover, measurement bias caused by harsh underwater environments is alleviated with a time-varying compensation strategy. Simulation results validate the superiority of CLADI by comparisons with the alternative ones.

Acknowledgments: This work was supported in part by the National Natural Science Foundation of China (62203299), and the Oceanic Interdisciplinary Program of Shanghai Jiao Tong University (SL2022MS008, SL2020ZD206, SL2022MS010).

References

[1] Z. Zhou, J. Liu, and J. Yu, "A survey of underwater multi-robot systems," *IEEE/CAA J. Autom. Sinica*, vol. 9, no. 1, pp. 1–18, Jan. 2022.

[2] R. A. Khalil, N. Saeed, M. I. Babar, T. Jan, and S. Din, "Bayesian multidimensional scaling for location awareness in hybrid-internet of underwater things," *IEEE/CAA J. Autom. Sinica*, vol. 9, no. 3, pp. 496–509, Mar. 2022.

[3] Y. Li, L. Liu, W. Yu, Y. Wang, and X. Guan, "Noncooperative mobile target tracking using multiple AUVs in anchor-free environments," *IEEE Internet Things J.*, vol. 7, no. 10, pp. 9819–9833, Oct. 2020.

[4] L. Paull, S. Saeedi, M. Seto, and H. Li, "AUV navigation and localization: A review," *IEEE J. Ocean. Eng.*, vol. 39, no. 1, pp. 131–149, Jan. 2014.

[5] Y. Shen, H. Wymeersch, and M. Z. Win, "Fundamental limits of wideband localization—Part II: Cooperative networks," *IEEE Trans. Inf. Theory*, vol. 56, no. 10, pp. 4981–5000, Oct. 2010.

[6] Y. Xiong, N. Wu, Y. Shen, and M. Z. Win, "Cooperative localization in massive networks," *IEEE Trans. Inf. Theory*, vol. 68, no. 2, Feb. 2022.

[7] S. Wang, L. Chen, D. Gu, and H. Hu, "Cooperative localization of AUVs using moving horizon estimation," *IEEE/CAA J. Autom. Sinica*, vol. 1, no. 1, pp. 68–76, Jan. 2014.

[8] J. Lien, U. J. Ferner, W. Srichavengsup, H. Wymeersch, and M. Z. Win, "A comparison of parametric and sample-based message representation in cooperative localization," *Int. J. Navig. Observ.*, vol. 2012, pp. 1–10, Jul. 2012.

[9] F. Meyer, O. Hlinka, and F. Hlawatsch, "Sigma point belief propagation," *IEEE Signal Process. Lett.*, vol. 21, no. 2, pp. 145–149, Feb. 2014.

[10] Y. Li, Y. Wang, W. Yu, and X. Guan, "Multiple autonomous underwater vehicle cooperative localization in anchor-free environments," *IEEE J. Ocean. Eng.*, vol. 44, no. 4, pp. 895–911, Oct. 2019.

[11] Y. Li, B. Li, W. Yu, S. Zhu, and X. Guan, "Cooperative localization based multi-AUV trajectory planning for target approaching in anchor-free environments," *IEEE Trans. Veh. Technol.*, vol. 71, no. 3, pp. 3092–3107, Mar. 2022.

[12] M. Yuan, Y. Li, Y. Li, S. Pang, and J. Zhang, "A fast way of single-beacon localization for AUVs," *Appl. Ocean Res.*, vol. 119, p. 103037, Feb. 2022.

[13] X. Liu, J. Yin, S. Zhang, B. Ding, S. Guo, and K. Wang, "Range-based localization for sparse 3-D sensor networks," *IEEE Internet Things J.*, vol. 6, no. 1, pp. 753–764, Feb. 2019.